Published in final edited form as:
Hypertension. 2014 June ; 63(6): 1345–1353. doi:10.1161/HYPERTENSIONAHA.113.02804.

New therapy *via* targeting androgen receptor in monocytes/macrophages to battle atherosclerosis

Chiung-Kuei Huang[a,*], **Haiyan Pang**[b,a,*], **Lin Wang**[b,*], **Yuanjie Niu**[b], **Jie Luo**[a], **Eugene Chang**[c], **Janet D. Sparks**[a], **Soo Ok Lee**[a,#], and **Chawnshang Chang**[a,d,#]

[a]George Whipple Lab for Cancer Research, Departments of Pathology, Urology, Radiation Oncology, and the Wilmot Cancer Center, University of Rochester Medical Center, NY 14642, USA

[b]Chawnshang Chang Sex Hormone Research Center and The Kidney and Blood Purification Center, Tianjin Institute of Urology, Tianjin Medical University, Tianjin 300211, China

[c]Aab Cardiovascular Research Institute and Department of Pathology, University of Rochester Medical Center, NY 14642, USA

[d]Sex Hormone Research Center, China Medical University/Hospital, Taichung 404, Taiwan

Abstract

The male gender has a higher risk to develop the coronary artery diseases (CAD) including atherosclerosis. The androgen receptor (AR) is expressed in several atherosclerosis associated cell types, including monocytes/macrophages, endothelial cells (ECs), and smooth muscle cells (SMCs), but its pathophysiological role in each cell type during the development of atherosclerotic lesions remains unclear. Using the Cre-loxP system, we selectively knocked out AR in these three cell types and the resultant ARKO mice, monocyte/macrophage ARKO (MARKO), EC-ARKO (EARKO), and SMC-ARKO (SARKO), were then crossed with the low density lipoprotein receptor (LDLR) deficient (LDLR$^{-/-}$) mice to develop MARKO-LDLR$^{-/-}$, EARKO-LDLR$^{-/-}$, and SARKO-LDLR$^{-/-}$ mice for the study of atherosclerosis. The results showed that the MARKO-LDLR$^{-/-}$ mice had reduced atherosclerosis compared to the wild type (WT-LDLR$^{-/-}$) control mice. However, no significant difference was detected in EARKO-LDLR$^{-/-}$ and SARKO-LDLR$^{-/-}$ mice compared to WT-LDLR$^{-/-}$ mice, suggesting that the AR in monocytes/macrophages, and not in ECs and SMCs, plays a major role to promote atherosclerosis. Molecular mechanism dissection suggested that AR in monocytes/macrophages up-regulated the TNF-α, ITGβ2, and LOX-1 molecules that are involved in 3 major inflammation related processes in atherosclerosis, including monocytes/macrophages migration and adhesion to HUVECs cells, and subsequent foam cell formation. Targeting AR *via* the AR degradation enhancer, ASC-J9®, in WT-LDLR$^{-/-}$ mice showed similar effects as seen in MARKO-LDLR$^{-/-}$ mice with little influence on lipid profile. In conclusion, the AR in monocytes/macrophages plays key roles in

[#]Corresponding Authors: Chawnshang Chang, chang@urmc.rochester.edu, Phone: 1-585-273-4500, Fax: 1-585-756-4133.
[*]Contributed equally

Conflict of Interest

ASC-J9® was patented by the University of Rochester, the University of North Carolina, and AndroScience, and then licensed to AndroScience. Both the University of Rochester and C.C. own royalties and equity in AndroScience.

atherosclerosis and targeting AR with ASC-J9® may represent a new potential therapeutic approach to battle atherosclerosis.

Keywords

atherosclerosis; receptor; androgen; monocytes/macrophages

INTRODUCTION

The male gender is one of the risk factors for coronary artery disease (CAD) and the average life expectancy for men with CAD is about 8 years less than that of women with CAD. Atherosclerosis is the primary cause of CAD, and it therefore represents the most common cause of morbidity and mortality from CAD worldwide [1]. Atherosclerosis is an inflammatory disease, characterized by lipid and macrophage depositions in the arterial wall [2]. The atherosclerosis is initiated by the activation of endothelial cells (ECs), leading to high expression of adhesion molecules for recruiting inflammatory cells [3]. Macrophage colony-stimulating factor induces monocytes to enter the plaque to differentiate into macrophages and foam cells, which is a critical step for the atherosclerosis [4]. In the plaque centers, foam cells and extracellular lipid droplets form a core region, which is surrounded by a cap of smooth muscle cells (SMCs) and a collagen-rich matrix. T cells, macrophages, and mast cells infiltrate the lesion and are particularly abundant in the shoulder region of the plaque where the atheroma grows. Many of the immune cells exhibit signs of activation and produce inflammatory cytokines [4].

Almost all of the previous studies were focused on the androgen effect on atherosclerosis as androgen is considered to be the main factor for male gender risk in atherosclerosis [5]. However, several recent results demonstrated a protective role of androgens [6, 7].

Compared with the effect of androgen, few studies have been done to reveal the androgen receptor (AR) effect on atherosclerosis. AR is activated by binding of androgens [8, 9], but it can also exert its function without the binding of androgen [10]. Therefore, it becomes obvious that the AR effect is not always the same as the androgen effect. One of the recent findings from wound healing studies demonstrated that the AR knockout (ARKO) effect is critical in mediating the suppressive effect in wound healing yet such AR effects could not be reversed by androgen treatment [11], suggesting that AR could function through androgen-independent pathways. Ikeda *et al* [12] recently investigated the effect of androgen/AR on atherosclerosis using the ApoE$^{-/-}$ derivative of the total AR knockout mice (GARKO-ApoE$^{-/-}$), however, their studies failed to distinguish the effect of androgen *vs* AR since their mouse model lacked both AR and androgen (serum testosterone dropped to almost an undetectable level).

Based on the inflammatory characteristic of atherosclerosis and the role of AR in enhancing inflammatory response, we hypothesized that AR would promote the progression of atherosclerosis and the AR in monocytes/macrophages might exert the primary function. In this study, cell-specific ARKO male mice were used to demonstrate that the AR in monocytes/macrophages is critical in atherosclerosis.

MATERIALS AND METHODS

Please see supplemental information for materials and methods.

RESULTS

Atherosclerotic plaques were increased in GARKO-LDLR$^{-/-}$ mice but decreased in MARKO-LDLR$^{-/-}$ mice compared to the WT-LDLR$^{-/-}$ littermate control mice

Using the Cre-loxP system, we either knocked out AR ubiquitously or selectively in 3 major cell types associated with atherosclerosis: monocytes/macrophages, ECs, and SMCs, and the resultant monocytes/macrophage AR knockout (MARKO), ECs-ARKO (EARKO), and SMC-ARKO (SARKO) mice were then crossed with the low density lipoprotein receptor (LDLR) deficient (LDLR$^{-/-}$) mice to develop GARKO-LDLR$^{-/-}$, MARKO-LDLR$^{-/-}$, EARKO-LDLR$^{-/-}$, and SARKO-LDLR$^{-/-}$ mice. Supplemental Fig. S1a shows the genotyping results of 4 types of the generated ARKO mice and Supplemental Fig. S1b shows the depletion of AR in the bone marrow derived macrophages obtained from MARKO-LDLR$^{-/-}$ mice. No significant change in body weight was observed in the MARKO-LDLR$^{-/-}$ mice, but we observed increases in body weight in the other two types of mice (EARKO-LDLR$^{-/-}$, and SARKO-LDLR$^{-/-}$) (Supplemental Fig. S1c)

After atherosclerosis was developed by feeding mice with high fat diet (HFD) for 16 weeks, aortas were excised from each group of mice and stained with Oil-red-O to visualize atherosclerotic plaques. Compared to the WT-LDLR$^{-/-}$ littlemate control mice, the GARKO-LDLR$^{-/-}$ showed increased atherosclerotic plaques and reduced androgen levels, which are consistent with previous findings (Fig. 1a–d) [13]. However, the MARKO-LDLR$^{-/-}$ mice showed significantly less atherosclerosis (25.9% reduction, p value <0.001, n=9) without an altered androgen level *as* compared to the WT-LDLR$^{-/-}$ littermate control mice (Fig. 2a, b, and e). In contrast, we found little differences in plaque areas in the EARKO-LDLR$^{-/-}$ and SARKO-LDLR$^{-/-}$ mice as compared to their littermate controls. The results indicate that there are no significant differences in androgen level among EARKO-LDLR−/−, SARKO-LDLR−/−, and their littermate controls (Fig. 2a, b, and f)). We then performed hematoxylin and eosin (H&E) staining of aortic tissues of these mice and detected reduced plaque area in the MARKO-LDLR$^{-/-}$ mice (38% reduction, p value <0.001, n=6) compared to the littermate control mice (n=5) (Fig. 2c, quantification of relative plaque areas were shown in 2d).

Together, the results of these studies using the LDLR$^{-/-}$ derivatives of the 4 different ARKO mice demonstrated that the AR in monocytes/macrophages, but not in ECs and SMCs, played an important role in the promotion of atherosclerosis.

Depletion of AR in monocytes/macrophages reduces monocytes infiltration into the aorta plaque area

A crucial step in atherosclerosis is an infiltration of monocytes into the sub-endothelial cells of the arteries where they differentiate into macrophages and become functionally active[14]. We therefore investigated monocytes infiltration in aortic tissues of the MARKO-LDLR$^{-/-}$ and WT-LDLR$^{-/-}$ littermate control mice by staining tissues with the monocyte specific

antibody, Mac-3. We found that the Mac-3 positively stained cell numbers (represented as positively stained cell %) were significantly decreased in the MARKO-LDLR$^{-/-}$ mice (5.28 ± 2.11%, n=7) compared to their littermate control mice (20.57 ± 4.42%, n=6) (Fig. 3a).

We also examined collagen deposition in aortas of MARKO-LDLR$^{-/-}$ and WT-LDLR$^{-/-}$ mice *via* Masson Trichrome staining, and results demonstrated significantly lower collagen deposition in the MARKO-LDLR$^{-/-}$ mice (10.14 ± 1.08%, n=5) compared to the littermate control mice (14.48 ± 1.28%, n=5) (Fig. 3b).

We further investigated whether invaded SMCs numbers were modulated by the AR knockout in monocytes/macrophages, and found that the α-smooth muscle actin (α-SMA) positively stained SMCs numbers were increased in the MARKO-LDLR$^{-/-}$ mice (28.70% ± 1.94%, n=5) compared to the control littermate mice (12.37 ± 1.71%, n=6) (Fig. 3c). This suggested that higher numbers of the migrated SMCs may stabilize the plaques leaving them less susceptible to rupture [15, 16]. Therefore, we believe that the AR knockout in monocytes/macrophages might contribute to the stability of plaques as shown by the increased numbers of the invaded SMCs in MARKO-LDLR$^{-/-}$ mice, thereby protecting mice from developing into the acute coronary syndrome (ACS).

Together, results of Fig. 3a–c concluded that the loss of AR in monocytes/macrophages resulted in decreased infiltrating monocytes/macrophages to the sub-endothelium of arteries with decreased collagen deposition and increased SMCs, and all these combined effects led to the suppression of atherosclerosis.

AR in monocyte THP-1 cells promoted their migration and adhesion to HUVECs cells and foam cell formation

To further confirm the above *in vivo* findings, we applied *in vitro* assays to show the AR role in monocytes/macrophages in promoting atherosclerosis. We first investigated whether the AR expression in monocytes influences their migration to ECs. The monocyte THP-1 cells were infected with lentivirus carrying either scramble control sequence or AR-siRNA and Fig. 4A-a (upper) shows successful knockdown of AR in these cells. In the migration assay, the THP-1 cells, either the AR knocked down (THP-1siAR) or the scramble control (THP-1sc) cells, were placed in the upper chamber while the conditioned media (CM) of HUVECs were placed in the lower chamber of transwell plates as shown in Fig. 4A-a (lower) cartoon. We found that the migration of the THP-1siAR cells was suppressed, when compared to the THP-1sc cells (Fig 4A-b). However, when we manipulated AR expression in HUVECs and used the CM of the AR expressing and depleted HUVECs in the tests, migration of THP-1 cells was not influenced significantly (data not shown), suggesting that AR expression in monocytes, and not in ECs, is critical in mediating this migration process.

We also tested adhesion of THP-1 cells onto HUVECs (a cartoon shown in upper panel of Fig. 4A-c). Similarly, we used THP-1-siAR and THP-1sc cells in the test and tagged THP-1 cells with green fluorescence dye (GFP) before the reaction so that the adhered GFP-labeled cells can easily be detected (middle panel). After incubation of two types of cells for 2 hrs at 37 °C, numbers of the adhered fluorescent THP-1 cells were counted. Similarly to the migration test, we found that adhesion of the THP-1siAR onto HUVECs was significantly

reduced (60%) compared to the THP-1sc (Fig. 4A-c lower panel; quantification, right panel, representative images in Supplemental Fig S2a). However, the manipulation of AR expression in HUVECs did not influence adhesion of THP-1 cells onto HUVECs significantly (data not shown). These results also suggest that AR expression in monocytes, and not in ECs, is critical in mediating this migration process and in promoting the adhesion process.

In addition of migration and adhesion, foam cell formation is the 3rd key step during atherosclerosis development[17]. Therefore, we tested whether the AR expression in THP-1 cells can also affect this process. THP-1siAR and THP-1sc cells, were treated with mouse derived colony stimulating factor (M-CSF) to stimulate differentiation of monocytes into macrophages and these resultant macrophages were subsequently treated with oxidized LDL (oxLDL) to induce foam cell formation. After staining of foam cells with Oil-red-O, the positively stained cells numbers were compared. As shown in Fig. 4A-d, the THP-1siAR cells have significantly reduced foam cell formation (11.89 ± 2.18%) as compared to the THP-1sc control cells (17.65 ± 1.72%), indicating that the AR in THP-1 cells also plays a stimulatory role in this process.

Taken together, Fig. 4A results suggest that the AR in monocytes/macrophages plays positive roles in promoting the 3 major inflammation associated processes in atherosclerosis: (i) migration, (ii) adhesion of monocytes to ECs, and (iii) subsequent foam cell formation.

Key AR-modulated molecules that affect migration of monocytes to ECs in THP-1 cells

We next investigated the molecular mechanisms by which the AR in monocytes/ macrophages promote the three inflammation associated processes *via* modulation of expressions of the target molecules of these processes.

Among the migration related molecules including TNF-α, IL-6, CCL2, and CCR2 we assayed, we found the mRNA expressions of TNF-α and IL-6 were the most significantly inhibited in THP-1siAR cells compared to THP-1sc cells (Fig. 4B-a). We then selected TNF-α for further investigation. As shown in Fig. 4B-b, we found that the secreted TNF-α protein was decreased dramatically in THP-1siAR cells compared to the THP-1sc cells, confirming the positive regulation of AR in TNF-α expression at both protein and mRNA levels.

We then asked if AR could modulate TNF-α at transcriptional level *via* ChIP assay. The results showed that the AR could bind to the androgen-response-element (ARE) (TNF promoter ARE1: +36~+41, ARE2: +50~+55) on the 5′ promoter region of TNF-α (Fig. 4B-c), and the luciferase assay also confirmed AR could induce TNF-α expression at transcriptional level (Fig. 4B-d).

We further applied functional assays to test if blocking TNF-α *via* a neutralizing antibody of TNF-α could suppress the AR effect in promoting migration of THP-1 cells into ECs. As shown in Fig. 4B-e, addition of TNF-α neutralizing antibody reduces THP-1-sc cells migration to the level of the THP-1-siAR cells, indicating that TNF-α is indeed critical in mediating the promoter role of AR in this process.

We also examined whether the TNF-α expression is reduced in the aortic tissues of the MARKO-LDLR$^{-/-}$ mice compared to their WT-LDLR$^{-/-}$ littermate control mice and found significantly reduced expressions of TNF-α in aortic tissues of MARKO-LDLR$^{-/-}$ mice compared to the WT-LDLR$^{-/-}$ littermate control mice (Fig. 4B-f), confirming the *in vitro* effect of AR modulation of TNF-α for promoting monocytes/macrophages migration to ECs.

Key AR-modulated molecules that affect adhesion of monocytes to ECs in THP-1 cells

Next we surveyed molecules that have been documented to play important roles in the adhesion process [15, 16], and found that the expression of integrin family members (ITGαM, αV, β1, β2) and PSGL-1 was suppressed in THP-1siAR cells compared to the THP-1sc control cells (Fig. 4C-a). We further dissected the molecular mechanism how AR could modulate ITGβ2 in the adhesion process, and confirmed AR could modulate ITGβ2 expression at both mRNA and protein levels (Fig. 4C-a,b).

We further examined AR modulation in ITGβ2 expression at the transcriptional level, and found that AR could bind to ARE (AGACCAnnnTGATCA, location −4462~−4447) on the 5′ promoter region of ITGβ2 *via* ChIP assay (Fig. 4C-c). The luciferase assay further confirmed AR could induce ITGβ2 expression at the transcriptional level in the 293T cells (Fig. 4C-d).

When we introduced the neutralizing antibody of ITGβ2 into the culture, we were able to inhibit adhesion of THP-1sc cells, but not the THP-1siAR cells (Fig. 4C-e, **representative images in** supplemental Fig. S2b), indicating that the ITGβ2 molecule is critical in this AR-mediated adhesion process.

Finally, we examined ITGβ2 expression in the aortic tissues of the MARKO-LDLR$^{-/-}$ mice and their WT-LDLR$^{-/-}$ littermate control mice, and found significantly reduced ITGβ2 expression in aortic tissues of MARKO-LDLR$^{-/-}$ mice compared to their littermate control mice (Fig. 4C-f), which also confirmed the AR mediated reduction of ITGβ2 *in vivo*.

Key AR-modulated molecules that affect foam cell formation in THP-1 cells

We then investigated the target molecules in foam cell formation process, such as LOX-1, LAL, and ACAT, in THP-1siAR and THP-1sc cells, and found that expressions of these 3 molecules were suppressed in the THP-1siAR cells (Fig. 4D-a). Further analysis of LOX-1 expression in THP-1siAR and THP-1sc cells showed lower mRNA expression of LOX-1 in THP-1-siAR cells compared to the THP-1sc cells (Fig. 4D-b).

We also used the ChIP assay to determine if AR could modulate LOX-1 expression at the transcriptional level, and the results showed that AR could bind to ARE (ATAAAAnnnTGTTTT, location −4209~−4194) on the 5′ promoter region of LOX-1 (Fig. 4D-c). As expected, the luciferase assay also confirmed AR could induce LOX-1 expression at the transcriptional level (Fig. 4D-d).

We further tested whether the blocking of LOX-1 by treating the THP-1-siAR and THP-1sc cells with the LOX-1neutralizing antibody could inhibit foam cell formation. As shown in

Fig. 4D-e, the foam cell formation was significantly inhibited upon antibody treatment in THP-1sc cells, but not in THP-1siAR cells.

We then examined LOX-1 expression in the aortic tissues of the MARKO-LDLR$^{-/-}$ and their WT-LDLR$^{-/-}$ littermate control mice and found significantly reduced expressions of LOX-1 in aortic tissues of MARKO-LDLR$^{-/-}$ mice compared to their littermate control mice (Fig. 4D-f), suggesting AR could go through modulation of LOX-1 expression to influence form cell formation *in vivo*.

Together, results from Fig. 4 show that the AR in monocytes/macrophages might play a stimulatory role to promote atherosclerosis *via* multiple modulations of various key molecules, which might explain why we could detect decreased plaque formation in the MARKO-LDLR$^{-/-}$ mice (see Fig. 2).

Targeting monocyte/macrophage AR with ASC-J9® to battle atherosclerosis

We then asked how can we target monocytes/macrophages AR in the body to mimic the MARKO-LDLR$^{-/-}$ mice effect and use that strategy as a potential new therapeutic approach to battle atherosclerosis. ASC-J9® is an AR degradation enhancer, which functions through the proteasome machinery to selectively degrade AR. ASC-J9® could increase Akt modulated AR and Mdm2 interaction and recruit the proteasome complex to enhance AR's degradation [18]. The earlier studies on wound healing demonstrated that ASC-J9® was able to selectively degrade AR in monocytes/macrophages, and mimicked the MARKO mice effect with improved wound healing [11].

We first tested the *in vitro* ASC-J9® effects in inhibiting three processes: migration and adhesion of monocytes onto ECs and subsequent foam cell formation. Our results showed that ASC-J9® could enhance AR protein degradation in THP-1 cells starting at 2.5 μM concentration (Fig. 5a). When we used 5 μM ASC-J9® to test its effect on THP-1 cell migration into HUVECs, we found significant reduction in THP-1 cells migration (Fig. 5b). We then tested ASC-J9® effect on the adhesion of THP-1 cells onto HUVECs. As shown in Fig. 5c, THP-1 cells adhesion was also significantly reduced upon ASC-J9® treatment (representative images in supplemental Fig. S2c). We further examined ASC-J9® effects on foam cell formation and obtained similar results showing suppressive effects of ASC-J9® (2.5 to 10 μM) (Fig. 5d).

We then extended our studies of ASC-J9® effects into *in vivo* mice studies. ASC-J9® was injected i.p every other day (75 mg/kg/day) into the 16 weeks old WT-LDLR$^{-/-}$ mice, 8 wks after starting HFD feeding and continued for 8 wks. In parallel, control littermates received vehicle only. After a total of 16 weeks HFD feeding, mice were sacrificed and atherosclerosis parameters were analyzed. Interestingly, the results showed that the WT-LDLR$^{-/-}$ mice treated with ASC-J9® have significantly decreased plaque area (25.1 ± 4.9%, n=11) compared to the vehicle control mice (19.2 ± 5.7%, n=5) (Fig. 6a). We then examined whether the treatment with ASC-J9® leads to decreased AR expression in macrophage. The IHC staining revealed that the expression of monocyte/macrophage AR (Fig. 6b) and macrophage infiltration (Fig. 6c) were significantly decreased in these ASC-J9® treated mice. Importantly, we found that mice treated with ASC-J9® still had normal body weight

with near normal serum testosterone and normal fertility, which is consistent with the previous results showing few side effects [11, 19].

Together, the results from *in vitro* cell lines (Fig. 5) and *in vivo* mice studies (Fig. 6) suggests that ASC-J9® may have a therapeutic potential to battle the atherosclerosis in the future.

DISCUSSION

In these studies we found that general AR knockout in LDLR−/− (GARKO-LDLR−/−) mice significantly increased atherosclerotic plaques, whereas AR knockout in monocytes/macrophages significantly reduced plaque area as shown in MARKO-LDLR$^{-/-}$ mice. However, the mice lacking AR in ECs and SMCs failed to show such effect, suggesting that the AR in monocytes/macrophages may play critical roles in promoting atherosclerosis. Interestingly, MARKO-LDLR−/− mice showed completely opposite results to the GARKO-LDLR−/− mice. Actually, there may be multiple factors contributing to these contrasting effects observed in GARKO-LDLR$^{-/-}$ *vs* MARKO-LDLR$^{-/-}$ mice on atherosclerosis. First, this may be explained by the serum testosterone level difference since the serum testosterone levels in the GARKO-LDLR$^{-/-}$ mice dropped dramatically, while the serum testosterone levels in the MARKO-LDLR$^{-/-}$ mice remained almost unchanged as compared to the WT-LDLR$^{-/-}$ littermate control mice. Early studies documented that testosterone therapy could lead to reduced cholesterol and LDL levels [20–23], and higher frequency of atherosclerosis was also observed in prostate cancer patients after receiving androgen deprivation therapy [24], suggesting androgens may play protective roles in atherosclerosis development. Our results showing GARKO-LDLR$^{-/-}$ mice with low level of serum testosterone developed atherosclerosis, yet MARKO-LDLR$^{-/-}$ mice with normal serum testosterone level developed little atherosclerosis are in agreement with these clinical data.

Second, we may explain the opposite atherosclerosis phenotypes of the GARKO-LDLR$^{-/-}$ and MARKO-LDLR$^{-/-}$ mice by lipid profile differences. When we investigated lipid levels in these two types of ARKO mice, it was shown that total cholesterol and triglyceride (TG) contents were significantly higher in GARKO-LDLR$^{-/-}$ mice than in the WT-LDLR$^{-/-}$ littermate control mice, while MARKO-LDLR$^{-/-}$ mice showed little change (Supplemental Fig. S3a and b). These results suggest that the higher levels of cholesterol and TG in GARKO-LDLR$^{-/-}$ mice might contribute to the higher rate of plaque formation.

The high lipid levels in GARKO-LDLR$^{-/-}$ mice may be due to the low testosterone levels. However, our earlier studies in GARKO mice of metabolism and the current findings in SARKO-LDLR−/− mice indicate that the higher lipid levels may not be independently affected by testosterone levels[25]. When we investigated whole lipid/glucose metabolism difference in GARKO mice, we observed that GARKO mice had high lipid levels, and these high lipid levels were not reversed when we treated the GARKO mice with androgen [25]. Next, we investigated in which tissues the AR knockout is critical in elevating lipid levels. We found that AR knockout in SMCs results in significant increases in triglyceride and cholesterol without altering androgen levels (Supplemental Fig. S3c). We also found that the AR knockout in neurons in the neuronal ARKO (NARKO) mice resulted in high lipid levels

and further revealed that the NARKO mice had induced hypothalamic insulin resistance, which, in turn, led to hepatic insulin resistance, lipid accumulation, and visceral obesity [26]. Therefore, it can be speculated that the higher lipid levels observed in the GARO-LDLR$^{-/-}$ mice may be related to the smooth muscle cellular and neuronal AR knockout in those mice. Although SARKO-LDLR−/− mice exhibit similar atherosclerotic plaques as the littermate controls, whether the atherosclerosis mouse model using the neuronal ARKO mice will lead to higher atherosclerosis similar to the GARKO-LDLR$^{-/-}$ mice needs to be investigated in the future to draw a solid conclusion.

No matter what the major factor is, it is obvious that targeting androgen/AR signaling in the whole body (as current androgen deprivation therapy does in prostate cancer patients using various anti-androgens to suppress androgen binding to AR in the whole body) may not be an effective way to suppress atherosclerosis and therefore, we need to develop a way to suppress monocytes/macrophages without affecting testosterone and lipid levels.

We, therefore, suggest the use of the AR degradation enhancer ASC-J9® as a new potential therapeutic approach to battle atherosclerosis with rationales as follows. (a) The ASC-J9® treated WT-LDLR$^{-/-}$ mice mimicked the MARKO-LDLR$^{-/-}$ mice effect, similar to the early study demonstrating ASC-J9® could degrade AR in macrophages to reach the therapeutic effect in macrophage-mediated wound healing [11]. (b) The ASC-J9® treated WT-LDLR$^{-/-}$ mice showed reduced plaque formation to a similar extent as observed in MARKO-LDLR$^{-/-}$ mice. (c) Mice treated with ASC-J9® show little change in serum testosterone [11] and AR could be degraded in selective cell types including macrophages, SMCs, prostate, and heart (Supplemental Fig. S4a). (d) *In vivo* data demonstrated that ASC-J9® treated mice have normal libido and sexual activity with normal fertility [11, 19, 27–29].

In summary, we conclude that targeting AR in monocyte/macrophages may be a new effective therapy to battle atherosclerosis that can be achieved by exploiting ASC-J9® in the therapeutic approach. Supplemental Fig. S5 cartoon explains our entire approach [11].

Perspectives

Atherosclerosis is an inflammatory and metabolic disease. AR plays important roles in metabolism and inflammation. AR promotes inflammatory responses as demonstrated by using castrated male mice and GARKO mice to show reduced inflammatory responses. However, androgen and AR signaling are very complicated in lipid and glucose metabolism and abnormal metabolism would increase lipid accumulation in the blood stream to cause atherosclerosis. In our previous studies, we have shown that neuron and hepatocyte specific ARKO mice have elevated lipid profiles, whereas adipocyte specific ARKO mice have decreased lipid profiles[30]. In the current study, we showed that MARKO mice have slightly lower lipid profiles, EARKO mice have no change regarding lipid profiles, but SARKO mice have surprisingly elevated lipid profiles, even higher than GARKO mice. From these results of many cell specific ARKO mice, it could be speculated that the changed lipid profiles of GARKO mice is a summation of AR effects on different kinds of cells that are involved in metabolism. It might not be easy to simply target AR in the whole body, since this would worsen the atherosclerosis progression. Luckily, we investigated an AR

degradation enhancer, ASC-J9®, and found that it has the potential to target AR in monocyte/macrophage to suppress atherosclerosis. Although ASC-J9® could suppress atherosclerosis progression, we actually do not know whether treatment with ASC-J9® could result in insulin resistance which has been shown by using GARKO and several cell specific ARKO mice. Future studies are needed in order to evaluate the safety of ASC-J9® before initiating in clinical studies.

Supplementary Material

Refer to Web version on PubMed Central for supplementary material.

Acknowledgments

We thank K. Wolf for help in editing the manuscript.

Source of funding

This work was supported by NIH Grants (CA127300 and CA156700) and Taiwan Department of Health Clinical Trial and Research Center of Excellence Grant DOH99-TD-B-111-004 (China Medical University, Taichung, Taiwan).

References

1. Eckardstein A, Wu FC. Testosterone and atherosclerosis. Growth Horm IGF Res. 2003; 13 (Suppl A):S72–84. [PubMed: 12914731]
2. Ross R. Atherosclerosis--an inflammatory disease. N Engl J Med. 1999; 340:115–126. [PubMed: 9887164]
3. Out R, Hoekstra M, Habets K, Meurs I, de Waard V, Hildebrand RB, Wang Y, Chimini G, Kuiper J, Van Berkel TJ, Van Eck M. Combined deletion of macrophage abca1 and abcg1 leads to massive lipid accumulation in tissue macrophages and distinct atherosclerosis at relatively low plasma cholesterol levels. Arterioscler Thromb Vasc Biol. 2008; 28:258–264. [PubMed: 18006857]
4. Hansson GK. Inflammation, atherosclerosis, and coronary artery disease. N Engl J Med. 2005; 352:1685–1695. [PubMed: 15843671]
5. Kaufman JM, Vermeulen A. The decline of androgen levels in elderly men and its clinical and therapeutic implications. Endocr Rev. 2005; 26:833–876. [PubMed: 15901667]
6. Svartberg J. Epidemiology: Testosterone and the metabolic syndrome. Int J Impot Res. 2007; 19:124–128. [PubMed: 16858366]
7. Qiu Y, Yanase T, Hu H, Tanaka T, Nishi Y, Liu M, Sueishi K, Sawamura T, Nawata H. Dihydrotestosterone suppresses foam cell formation and attenuates atherosclerosis development. Endocrinology. 2010; 151:3307–3316. [PubMed: 20427482]
8. Chang CS, Kokontis J, Liao ST. Molecular cloning of human and rat complementary DNA encoding androgen receptors. Science. 1988; 240:324–326. [PubMed: 3353726]
9. Heinlein CA, Chang C. Androgen receptor in prostate cancer. Endocr Rev. 2004; 25:276–308. [PubMed: 15082523]
10. Sugita S, Kawashima H, Tanaka T, Kurisu T, Sugimura K, Nakatani T. Effect of type i growth factor receptor tyrosine kinase inhibitors on phosphorylation and transactivation activity of the androgen receptor in prostate cancer cells: Ligand-independent activation of the n-terminal domain of the androgen receptor. Oncol Rep. 2004; 11:1273–1279. [PubMed: 15138566]
11. Lai JJ, Lai KP, Chuang KH, Chang P, Yu IC, Lin WJ, Chang C. Monocyte/macrophage androgen receptor suppresses cutaneous wound healing in mice by enhancing local tnf-alpha expression. J Clin Invest. 2009; 119:3739–3751. [PubMed: 19907077]
12. Ikeda Y, Aihara K, Yoshida S, Sato T, Yagi S, Iwase T, Sumitomo Y, Ise T, Ishikawa K, Azuma H, Akaike M, Kato S, Matsumoto T. Androgen-androgen receptor system protects against

angiotensin ii-induced vascular remodeling. Endocrinology. 2009; 150:2857–2864. [PubMed: 19196803]

13. Bourghardt J, Wilhelmson AS, Alexanderson C, De Gendt K, Verhoeven G, Krettek A, Ohlsson C, Tivesten A. Androgen receptor-dependent and independent atheroprotection by testosterone in male mice. Endocrinology. 2010; 151:5428–5437. [PubMed: 20861231]
14. Galkina E, Ley K. Immune and inflammatory mechanisms of atherosclerosis (*). Annu Rev Immunol. 2009; 27:165–197. [PubMed: 19302038]
15. Sukhova GK, Williams JK, Libby P. Statins reduce inflammation in atheroma of nonhuman primates independent of effects on serum cholesterol. Arterioscler Thromb Vasc Biol. 2002; 22:1452–1458. [PubMed: 12231565]
16. Libby P, Ridker PM, Maseri A. Inflammation and atherosclerosis. Circulation. 2002; 105:1135–1143. [PubMed: 11877368]
17. Glass CK, Witztum JL. Atherosclerosis. The road ahead. Cell. 2001; 104:503–516. [PubMed: 11239408]
18. Lai KP, Huang CK, Chang YJ, Chung CY, Yamashita S, Li L, Lee SO, Yeh S, Chang C. New therapeutic approach to suppress castration-resistant prostate cancer using asc-j9 via targeting androgen receptor in selective prostate cells. The American journal of pathology. 2013; 182:460–473. [PubMed: 23219429]
19. Yang Z, Chang YJ, Yu IC, Yeh S, Wu CC, Miyamoto H, Merry DE, Sobue G, Chen LM, Chang SS, Chang C. Asc-j9 ameliorates spinal and bulbar muscular atrophy phenotype via degradation of androgen receptor. Nat Med. 2007; 13:348–353. [PubMed: 17334372]
20. Saad F, Gooren LJ, Haider A, Yassin A. A dose-response study of testosterone on sexual dysfunction and features of the metabolic syndrome using testosterone gel and parenteral testosterone undecanoate. J Androl. 2008; 29:102–105. [PubMed: 17916569]
21. Saad F, Gooren L, Haider A, Yassin A. An exploratory study of the effects of 12 month administration of the novel long-acting testosterone undecanoate on measures of sexual function and the metabolic syndrome. Arch Androl. 2007; 53:353–357. [PubMed: 18357966]
22. Tenover JS. Effects of testosterone supplementation in the aging male. J Clin Endocrinol Metab. 1992; 75:1092–1098. [PubMed: 1400877]
23. Zgliczynski S, Ossowski M, Slowinska-Srzednicka J, Brzezinska A, Zgliczynski W, Soszynski P, Chotkowska E, Srzednicki M, Sadowski Z. Effect of testosterone replacement therapy on lipids and lipoproteins in hypogonadal and elderly men. Atherosclerosis. 1996; 121:35–43. [PubMed: 8678922]
24. Shahani S, Braga-Basaria M, Basaria S. Androgen deprivation therapy in prostate cancer and metabolic risk for atherosclerosis. The Journal of clinical endocrinology and metabolism. 2008; 93:2042–2049. [PubMed: 18349064]
25. Lin HY, Xu Q, Yeh S, Wang RS, Sparks JD, Chang C. Insulin and leptin resistance with hyperleptinemia in mice lacking androgen receptor. Diabetes. 2005; 54:1717–1725. [PubMed: 15919793]
26. Yu IC, Lin HY, Liu NC, Sparks JD, Yeh S, Fang LY, Chen L, Chang C. Neuronal androgen receptor regulates insulin sensitivity via suppression of hypothalamic nf-kappab-mediated ptp1b expression. Diabetes. 2013; 62:411–423. [PubMed: 23139353]
27. Yamashita S, Lai KP, Chuang KL, Xu D, Miyamoto H, Tochigi T, Pang ST, Li L, Arai Y, Kung HJ, Yeh S, Chang C. Asc-j9 suppresses castration-resistant prostate cancer growth through degradation of full-length and splice variant androgen receptors. Neoplasia. 2012; 14:74–83. [PubMed: 22355276]
28. Wu MH, Ma WL, Hsu CL, Chen YL, Ou JH, Ryan CK, Hung YC, Yeh S, Chang C. Androgen receptor promotes hepatitis b virus-induced hepatocarcinogenesis through modulation of hepatitis b virus rna transcription. Sci Transl Med. 2010; 2:32ra35.
29. Ma WL, Hsu CL, Wu MH, Wu CT, Wu CC, Lai JJ, Jou YS, Chen CW, Yeh S, Chang C. Androgen receptor is a new potential therapeutic target for the treatment of hepatocellular carcinoma. Gastroenterology. 2008; 135:947–955. 955 e941–945. [PubMed: 18639551]

30. Yu IC, Lin HY, Liu NC, Wang RS, Sparks JD, Yeh S, Chang C. Hyperleptinemia without obesity in male mice lacking androgen receptor in adipose tissue. Endocrinology. 2008; 149:2361–2368. [PubMed: 18276764]

Novelty and Significance

What is new?

This is the first study using cell specific ARKO mice to further clarify AR roles in three major types of cells that are involved in atherosclerosis initiation and progression.

What is relevant?

AR in monocytes/macrophages is important for atherosclerosis development but not AR in endothelial cells and SMCs. Although GARKO mice develop severe atherosclerosis, MARKO mice have reduced atherosclerotic plaques, indicating that targeting AR in monocytes/macrophages might have therapeutic effects on atherosclerosis. Using an AR degradation enhancer, ASC-J9®, to treat atherosclerotic mouse, we were able to show that ASC-J9® might be a potential therapeutic approach in atherosclerosis.

Summary

Monocytes/macrophages AR would promote atherosclerosis progression. Targeting monocytes/macrophages AR with ASC-J9®, an AR degradation enhancer could suppress atherosclerosis progression, and suggested targeting monocytes/macrophages AR as a novel therapeutic approach in atherosclerosis.

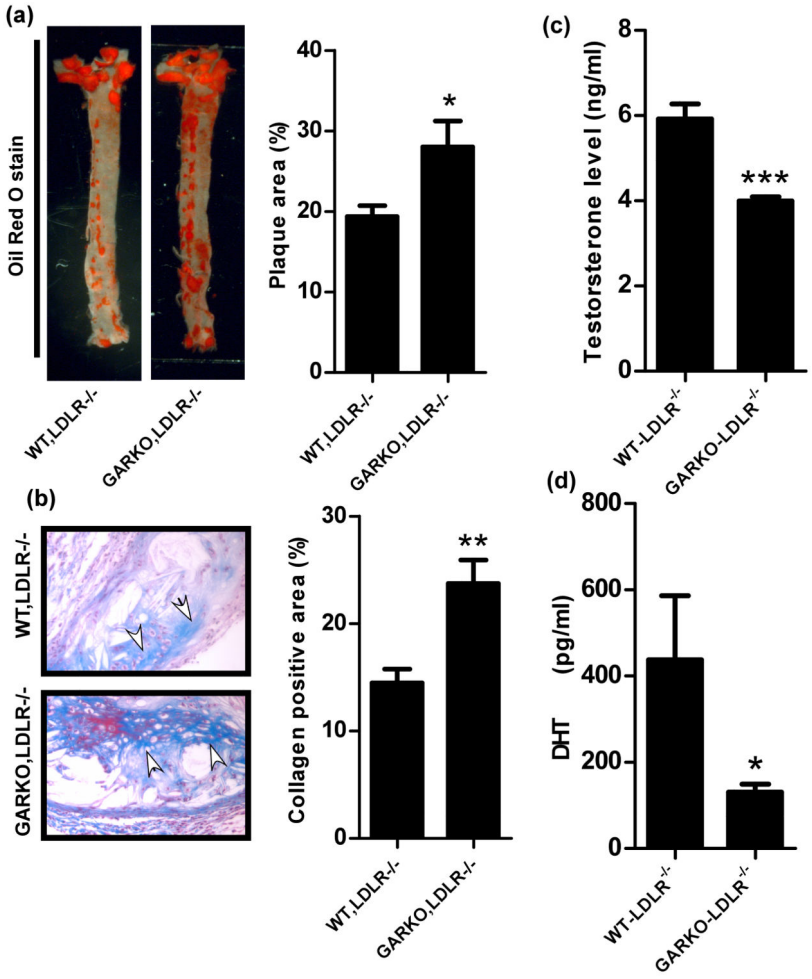

Fig. 1. Plaque formation was accelerated in GARKO-LDLR−/− mice compared to the WT-LDLR−/− littermate control mice

a. Plaque area was analyzed after staining with Oil red O stain. Graph on the right is quantitation result of plaque area over total area. b. Masson Trichrome staining was used to analyze collagen deposition in WT-LDLR−/− and GARKO-LDLR−/− mice. Graph on right shows the quantitation results of collagen positive area over total area. Arrows indicate collagen area (Blue color). Magnification, 400x. Androgens, (c) testosterone and (d) dihydrotestosterone (DHT) were measured using ELISA kit in WT-LDLR−/− and GARKO-LDLR−/− mice. *p<0.05, **p<0.01, and ***p<0.001.

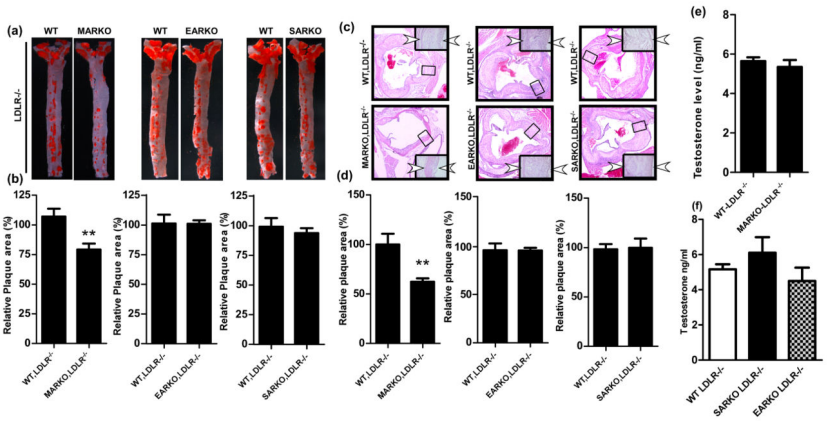

Fig. 2. Plaque area was reduced in the MARKO-LDLR$^{-/-}$ mice compared to the WT-LDLR$^{-/-}$ control mice, but not reduced in the EARKO-LDLR$^{-/-}$ and SARKO-LDLR$^{-/-}$ mice

a. Oil-red-O staining of aortas obtained from the MARKO-LDLR$^{-/-}$, EARKO-LDLR$^{-/-}$, and SARKO-LDLR$^{-/-}$ mice and their WT-LDLR$^{-/-}$ littermate control mice. Aorta were stained with Oil-red-O and positive red stained area indicates plaques formed. **b.** Quantitation results of positive plaque area over total area from a. **c.** H & E staining of aortic tissues of MARKO-LDLR$^{-/-}$, EARKO-LDLR$^{-/-}$, and SARKO-LDLR$^{-/-}$ mice and their WT-LDLR$^{-/-}$ littermate control mice. Magnification, 100x (inset, 400x). Two arrowheads indicate the plaque area. **d.** Quantitation of plaque area over total area from c. **e.** Testosterone levels were determined in MARKO-LDLR−/− mice and their WT-LDLR−/− littermate controls. **f.** Testosterone levels in WT-LDLR−/−, SARKO-LDLR−/−, and EARKO-LDLR−/− mice. $^{**}p<0.01$

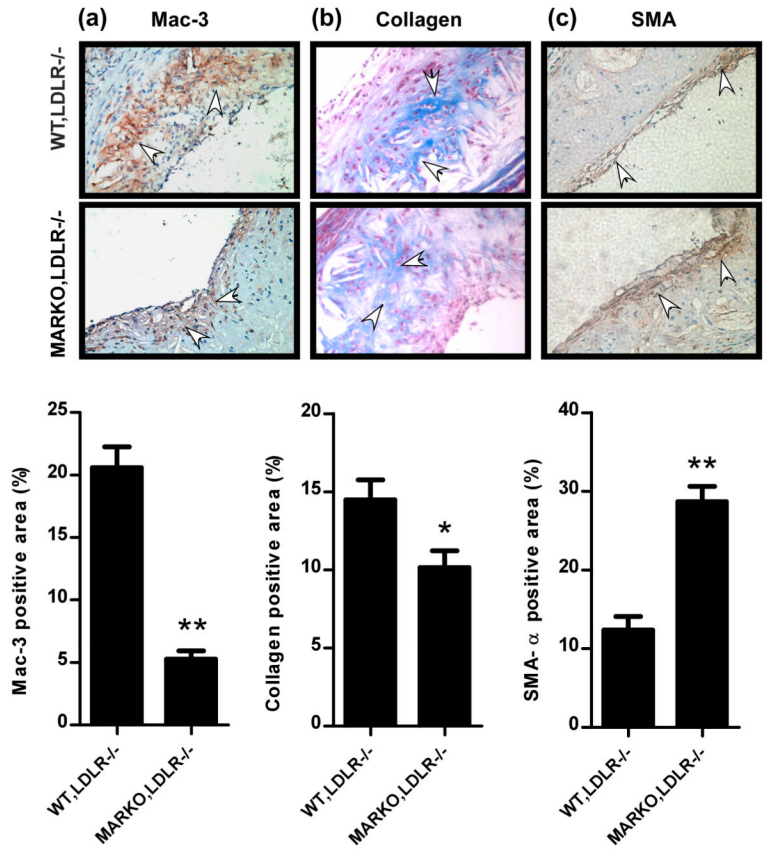

Fig. 3. Macrophage infiltration and collagen deposition were reduced, but SMCs invasion was increased in the MARKO-LDLR$^{-/-}$ mice compared to the WT-LDLR$^{-/-}$ mice

a. Aortic tissues of the MARKO-LDLR$^{-/-}$ and WT-LDLR$^{-/-}$ mice were stained with Mac-3 antibody. Arrows indicate stained Mac-3 positively stained cells. Magnification, 100x. Quantitation is showed below images $^{**}p<0.01$ **b.** Aortic tissues of the MARKO-LDLR$^{-/-}$ and WT,LDLR$^{-/-}$ mice were used in the Masson Trichrome staining. Arrows indicate positively stained cells. Magnification, 100x. Quantitation is shown below images. $^{*}p<0.05$ **c**. IHC staining of SMC invasion. Aortic tissues of the MARKO-LDLR$^{-/-}$ and WT-LDLR$^{-/-}$ mice stained with αSMA. Arrows indicate positively stained cells. Magnification, 100x. Quantitation is shown below images. $^{**}p<0.01$.

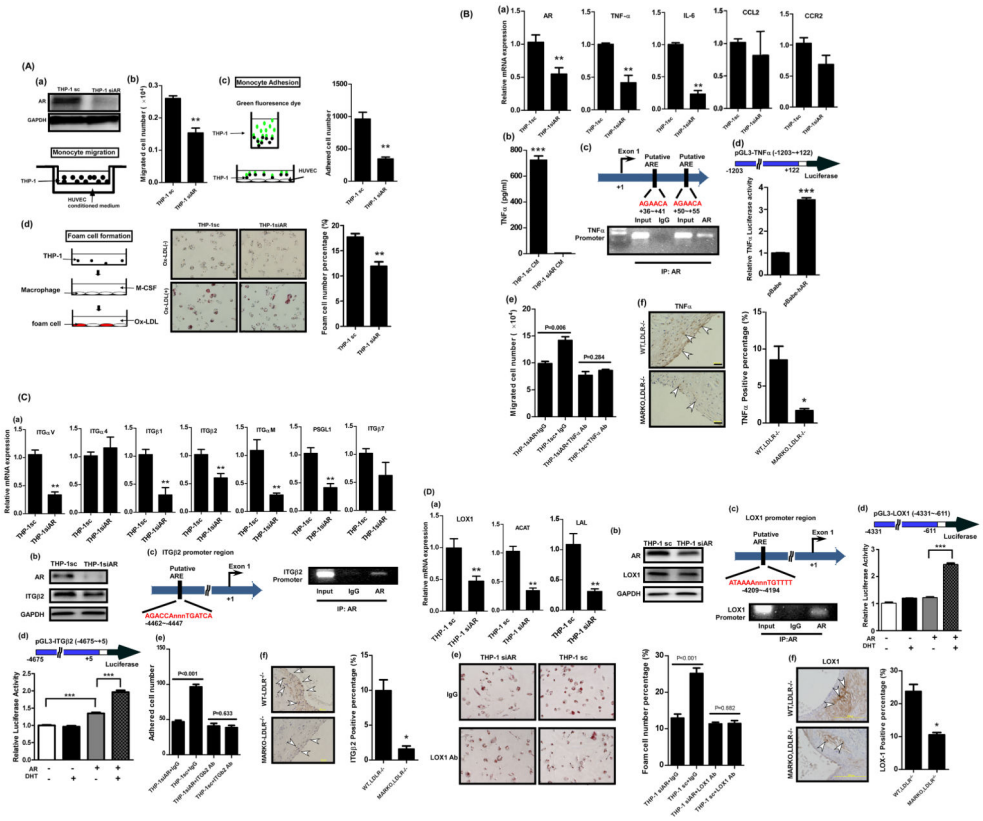

Fig. 4.

Fig. 4A. AR in THP-1 cells play a stimulatory role to promote the migration and adhesion to HUVECs and foam cell formation. a. THP-1siAR and THP-1sc, and HUVECs conditioned media (CM) were placed in transwell plates as described in the cartoon (lower panel). **b.** The migrated cells were stained and the positively stained cells numbers were measured. **p<0.01 **c.** THP-1siAR and THP-1sc, were tagged with GFP and then incubated with HUVECs. The adhered THP-1 cells with green fluorescence were counted. Quantitation is shown on the right. Magnification, 100x. **p<0.01 **d.** The THP-1siAR and THP-1sc cells were induced to differentiate into macrophage by M-CSF. The cells were then incubated with oxLDL to evaluate the ability of cells to uptake oxLDL (cartoon in left panel). At the end of reaction, cells were stained with filtered Oil-red-O (middle panel). Magnification, 100x. Quantitation is shown on the right. **p<0.01.

Fig. 4B. The AR in THP-1 cells promotes migration to HUVECs. a. qPCR analysis testing mRNA expression levels of candidate molecules involved in migration process. **p<0.01 **b**. ELISA test showing TNF-α secretion by the THP-1siAR and THP-1sc cells. ***p<0.001 **c.** ChiP assay. AR antibody was used to pull down TNFα promoter region which contains androgen response elements (AREs) (upper panel). **d.** TNFα promoter transactivation was measured using luciferase constructs containing AR binding sites of the promoter region of TNF-α molecule in the presence of pBabe vector only or pBabe-AR. HEK-293 cells were used in this assay. **e.** Blocking effect of migration of THP-1 cells to HUVECs upon incubation with the TNF-α antibody. **f.** IHC staining of TNF-α in aortic tissues obtained from the MARKO-LDLR$^{-/-}$ and WT-LDLR$^{-/-}$ mice. Arrowheads indicate

positive stained areas. Magnification, 100x. Quantitation is shown on the right. *p<0.05, **p<0.01, and ***p<0.001.

Fig. 4C. The AR in THP-1 cells promotes adhesion to HUVECs. a. qPCR analysis testing mRNA expression levels of candidate molecules involved in adhesion process, **p<0.01. **b**. Western blot analysis showing AR and ITGβ2 in the THP-1siAR and THP-1sc cells. GAPDH was used as control. **c.** ChiP assay. AR antibody was used to pull down ITGβ2 promoter region which contains AREs. **d.** ITGβ2 promoter transactivation was measured using luciferase construct containing ITGβ2 promoter region in the presence or absence of AR with or without DHT. HEK-293 cells were used in this assay. **e.** Blocking effect of adhesion of THP-1siAR and THP-1sc cells onto the HUVECs upon incubation with the ITGβ2 antibody. **f.** IHC staining of ITGβ2 in aortic tissues obtained from the MARKO-LDLR$^{-/-}$ and WT-LDLR$^{-/-}$ mice. Magnification, 400x. Arrowheads indicate positive stained area. Quantitation is shown on the right. *p<0.05, **p<0.01, and ***p<0.001.

Fig. 4D. The AR in macrophages promotes foam cell formation. a. qPCR analysis testing mRNA expression levels of candidate molecules involved in foam cell formation process. **p<0.01 **b.** AR and LOX-1 expression levels were determined using western blot in THP1-sc and THP1-siAR cells. GAPDH served as loading control. **c**. LOX-1 promoter region containing ARE (upper) was pulled down with AR antibody and amplified with primers specific targeting ARE region (lower). **d.** LOX-1 promoter region was constructed to pGL3 luciferase vector. The LOX-1 promoter transactivation was measured in the presence or absence of AR with or without DHT. **e.** Blocking effect on foam cell formation upon incubation with the LOX-1 antibody. Quantitation is shown on the right. **f.** IHC staining of LOX-1 in aortic tissues obtained from the MARKO-LDLR$^{-/-}$ and WT-LDLR$^{-/-}$ mice. Magnification, 100x. Quantitation is shown on the right. *p<0.05, **p<0.01, and ***p<0.001.

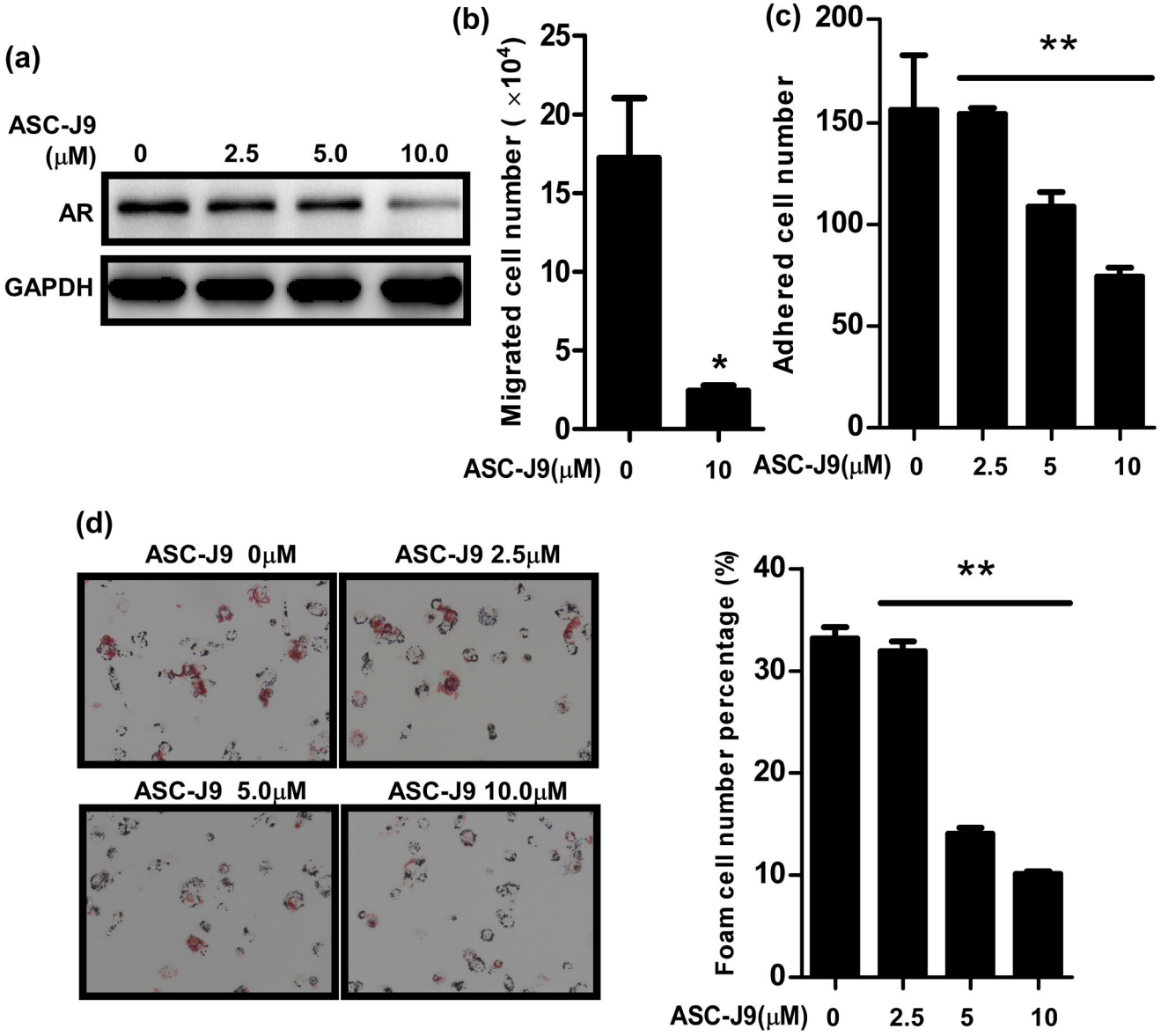

Fig. 5. ASC-J9® treatment blocked THP-1 cells migration and adhesion into HUVECs, and foam cell formation

a. Western blot analysis showing AR protein levels in THP-1 cells upon ASC-J9® treatment. **b.** *In vitro* test of ASC-J9® effect on migration of THP-1 cells into HUVECs. THP-1 cells were treated with ASC-J9® (10 μM) for 2 days and used for the migration experiment. **p*<0.05 **c.** *In vitro* test of ASC-J9® effect on adhesion of THP-1 cells onto HUVECs. ***p*<0.01 **d.** *In vitro* test of ASC-J9® effect on foam cell formation. THP-1 cells were treated with various concentrations of ASC-J9® for 2 days and used for the experiment. Quantitation is shown on the right. ***p*<0.01

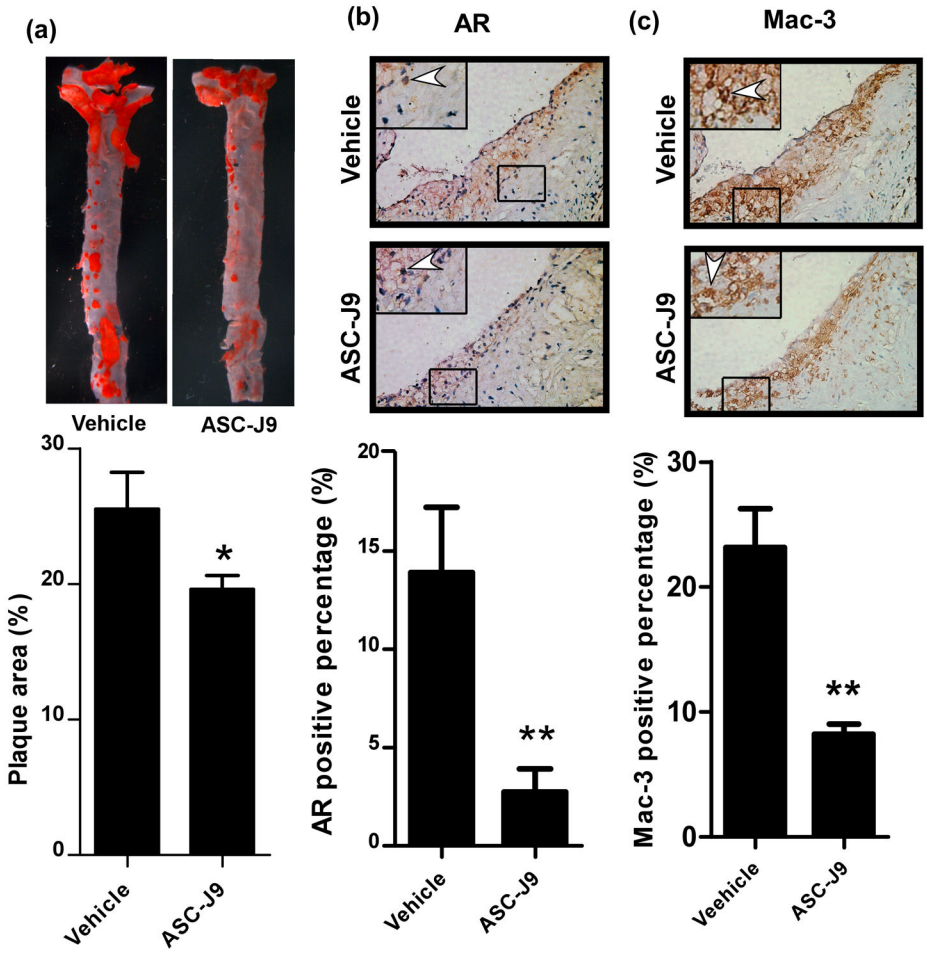

Fig. 6. Therapeutic effect of ASC-J9® in reducing atherosclerosis by inhibiting monocyte infiltration

a. ASC-J9® effects on plaque formation in mice. WT-LDLR$^{-/-}$ mice fed with HFD for 8 weeks were injected with ASC-J9® (75 mg/Kg body weight) every other day for another 8 weeks with continued HFD treatment. Quantitation is shown below images, *p<0.05 **b.** IHC staining results of AR in aortic tissues of vehicle and ASC-J9® treated mice. **c.** Mac-3 IHC staining results in aortic tissues of vehicle and ASC-J9® treated mice. For both **b** and **c**, magnification 100x, insets, 400x. Arrowheads indicate positive stained cells. Qnantitation is shown below images, **p<0.01.